Optimal Ball-end and Fillet-end Mills Selection for 3-Axis Finish Machining of Point-based Surface

Prasenjit Kayal[1, 2]

[1]School of Engineering (Mechanical), University of Birmingham, Edgbaston, Birmingham, B15 2TT, UK

[2]Present address: Engineering and Technology Development, Engineers India Limited, 1, Bhikaiji Cama Place, New Delhi 110066, India

Abstract

This paper presents an algorithm of optimal cutting tool selection for machining of the point-based surface that is defined by a set of surface points rather than parametric polynomial surface equations. As the ball-end and fillet-end mills are generally used for finish machining in a 3-axis computer numerical control machine, the algorithm is applicable for both cutters. The optimum tool would be as large as possible in terms of the cutter radius and/or corner radius which maximise (s) the material removal rate (i.e., minimise (s) the machining time), while still being able to machine the entire point-based surface without gouging any surface point. The gouging are two types: local and global. In this paper, the distance between the cutter bottom and surface points is used to check the local gouging whereas the shortest distance between the surface points and cutter axis is effectively used to check the global gouging. The selection procedure begins with a cutter from the tool library, which has the largest cutter radius and/or corner radius, and then adequacy of the point-density is checked to limit the accuracy of the cutter selection for the point-based surface within tolerance prior to the gouge checking. When the entire surface is gouge-free with a chosen cutting tool then the tool becomes the optimum cutting tool for a list of cutters available in the tool library. The effectiveness of the algorithm is demonstrated considering two examples.

Key Words: Optimal tool selection, point-based surface, ball-end mill, fillet-end mill, gouging

1. Introduction

3-axis computer numerically controlled (CNC) milling machines are commonly used to machine sculptured part surfaces [1] which are widely used in the aerospace, automobile and mould/die manufacturing industries [2, 3]. There are two stages in CNC machining: the rough and finish cut [4]. The

main purpose of the rough cut is to remove a large volume of material and leave only a small portion of raw stock to be removed with precision by the finish cut. The finishing operation aims to produce workpiece surfaces that conform to the design specification, and in particular have a high quality finish. The ball-end mill is inevitably used for finish machining because the centre of the ball always lies along the normal of the surface at a distance equal to the radius of the sphere, which makes CNC programming simpler. The algorithm of cutter path generation, interference checking and cutter compensation (2D) are easy to perform using the analytic geometric equation of a sphere [5]. The inherent limitation of the ball-end mill is that it rubs the material away in the vicinity of the cutter axis where the material is being removed at almost zero cutting speed irrespective of the spindle revolution. In order to achieve high material removal rate and improve surface finish, the fillet-end mill is preferred [6, 7]. The cutter path generation for free-form surface shapes represented by parametric polynomials has serious practical limitations [8]. Therefore, the generation of the CNC tool paths from the discretized point data without the need of parametric polynomial equations is an ongoing research issue. In the paper, the point-based approach is adopted for machining of sculptured surfaces that are defined by sets of surface points rather than explicit/implicit surface equations. Many researchers are nowadays proposing accurate and efficient tool path generation methods for the point-based surface [4, 9] with little consideration for selection of optimal tool size. The appropriate selection of the cutting tool is critical for ensuring the quality and efficiency of a CNC machining. It is difficult for human process planners to select the optimal cutter due to complex geometric interactions between the tool size and part shape. The cutting tool selection is a compromise between the two conflicting objectives [10]:

- Maximum material should be removed in each tool pass so that the overall machining time is reduced.
- The tool, while machining, should not gouge any surface point.

Although the former requires a larger tool, the latter restricts the size. A large cutter may cause local gouging on the part surface whereas a small cutter needs longer machining time and causes unnecessary tool wear [11]. In some cases, even the tool is locally gouge-free, the tool cannot enter into the entire surface region because of smaller tool body length and/or fixture size of tool holder assembly, which causes the global gouging. So the aim of the tool selection is to balance these conflicting requirements.

Research on automatic tool selection for CNC machining is limited. In the method proposed by Bala and Chang [12], roughing and finishing tools are selected using a circle fitting technique. Their method is limited to the machining of prismatic parts such as slots, steps, projections, etc. Yao *et al.* [13] give an algorithm for finding an optimal set of cutters for machining a set of $2\frac{1}{2}$D parts in terms of the real cutting and cutter changing time without consideration of the machined surface accuracy. Yang and

Han [14] present an optimal ball-end mil selection process for sculptured surfaces to be machined by a 3-axis CNC machine. Their method is an inline process that produces interference-free tool paths. Glaser *et al*. [15] develop a method that selects an appropriate size of the cutter based on collision-free milling process. A maximum effective cutting radius approach is proposed by Lee and Chang [11] to solve the cutter selection problem for multi-axis machining. Jensen *et al*. [16] present cutting tool selection methodology for five-axis finish surface machining based on curvature matching techniques.

Recently, OuYang *et al.* [17] propose an algorithm to determine the optimal ball-end mill size for 3-axis finish machining of the point-based surface using Voronoi diagram and Delaunay triangulation techniques, which are computationally expensive. Although the local gouging due to the cutter bottom is checked in their approach, the global gouging with the cutter body is not addressed. The disadvantage is that the accuracy of the tool size determination is very much dependent on the estimation of the normal vector at the surface point. Although the authors recognize that the accuracy of the determined tool sizes is heavily dependent on the density of the point data, no algorithm is reported to ensure adequate point density. To encounter the above difficulties, an automatic cutting tool selection methodology for ball-end and fillet-end mills is proposed in this paper for 3-axis CNC machining in order to provide gouge-free, efficient and accurate finish machining of any 3-D sculptured surface defined by a set of surface points. Before proposing the tool selection system, the effect of the cutter bottom size on the machining efficiency in terms of cutter path length is discussed in the following section.

2. Effect of cutter bottom on machining efficiency

The cutter bottom of the ball-end mill is geometrically hemisphere where the cutting takes place. For fillet-end mill, the cutter bottom consists of the circular bottom-disk of radius R_1 and toroidal part (corner radius of R_2), and the material removal takes place only on the toroidal part. For machining purpose, the cutter path planning is carried out by determining the step-forward distance (g_x) and step-interval distance (g_x) so that the combined machined surface error of the chordal deviation (e_x) due to g_x and cusp height (e_y) due to g_y limits within tolerance [18]. If the radii of curvature of the CL-curve are $(\rho_1 < 0)$, $(\rho_2 < 0)$ respectively in the forward and transverse directions and α_x, α_y are slope angles in respective directions then e_x and e_y for a ball-end mill of radius R are given by [18]:

$$e_x = \rho_1 + \sqrt{\rho_1^2 - \left(\frac{g_x}{2\cos\alpha_x}\right)^2} \tag{1}$$

$$e_y = \sqrt{\rho_2^2 - \left(\frac{g_y}{2\cos\alpha_y}\right)^2} + \sqrt{R^2 - \left(\frac{g_y}{2\cos\alpha_y}\right)^2} + (\rho_2 - R) \tag{2}$$

It is evident from Eqs. (1) and (2) that the chordal deviation does not depend on the cutter size but the cusp height (shown in figure 1) is very much dependent on the cutter radius. As the cusp height is very small compared to the cutter radius, Eq. (2) can be approximated by following expression:

$$g_y \approx \sqrt{\frac{8Re_y\rho_2}{\rho_2 - R}} \tag{3}$$

For a fillet-end mill, the distance g_y is generally within the cutter corner radius on the same side of the two cutters [19], as shown in figure 1(b) and the step-interval distance g_y is also obtained from equation (3) by substituting $R = R_2$ .The first partial derivative of g_y with respect to R is given by:

$$\frac{\partial g_y}{\partial R} = \frac{4e_y\rho_2^2}{(\rho_2 - R)^2}\sqrt{\frac{\rho_2 - R}{8\rho_2 Re_y}} \tag{4}$$

It is evident from Eq. (4) that $\frac{\partial e_y}{\partial R} > 0$ for a given cusp height $e_y > 0$. Therefore the step-interval distance g_y increases as the cutter radius R increases for a given cusp height e_y, which implies that less cutter paths are required to complete the surface machining if a larger radius or corner radius cutter is utilized [20]. Therefore, the largest cutter radius for the ball-end mill and the largest corner radius of the fillet-end mill from the tool library must be utilised to achieve the maximum machining efficiency in terms of cutter path length.

In order to find the influence of the bottom-disk radius R_1 on the material removal rate, the cutting speed v for a fillet-end mill is derived for a specified spindle speed N and slope angle θ according to figure 2:

$$v = 2\pi N\{R_1 + R_2\sin\theta\} \tag{5}$$

The first partial derivative of v with respect to R_1 is given by:

$$\frac{\partial v}{\partial R_1} = 2\pi N \tag{6}$$

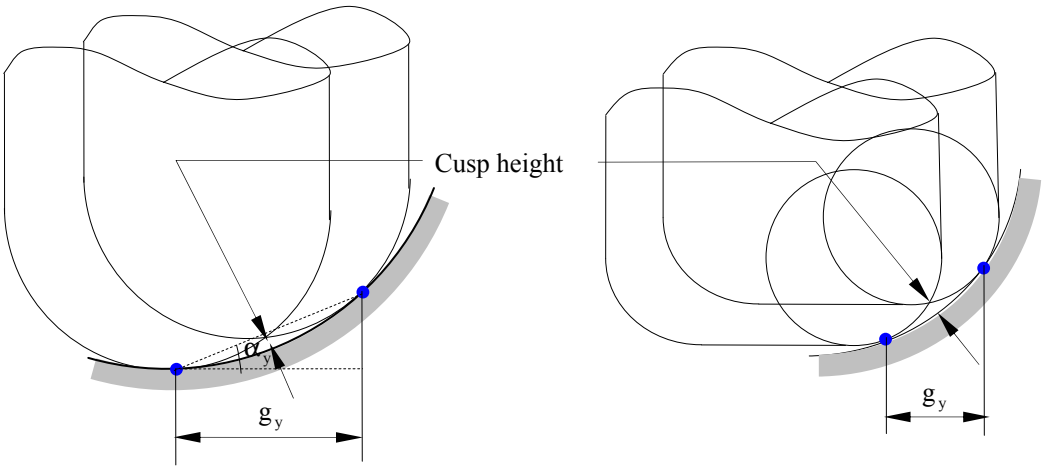

Fig. 1. Cusp height for (a) ball-end and (b) fillet-end mills

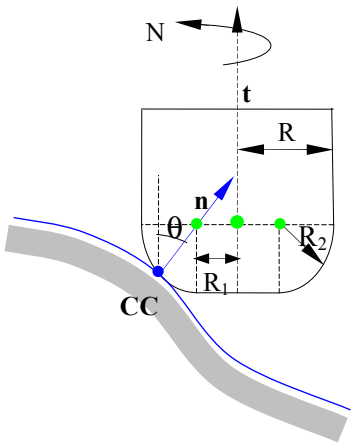

Fig. 2. Cutting speed

The Eq. (6) shows that $\frac{\partial v}{\partial R_1}$ = constant for a given spindle speed, which implies that the cutting speed increases as the disk radius increases when the corner radius is unchanged. Thus it can be concluded that when two fillet-end mills have the same corner radius, the fillet-end mill with larger disk radius enables to achieve higher cutting speed. As the step-interval distance (the cutter path length) does not depend on the bottom-disk radius, the primary emphasis is to be given for selecting the fillet end mill with higher corner radius and if the corner radii are the same then only the cutter with larger bottom-disk radius is considered for the tool selection.

3. Cutting tool selection system

The proposed cutting tool selection system for 3-axis finish machining is shown in figure 3, which can be used for any sculptured surface defined by a set of 3D surface points. The system consists of checking point density and checking for gouging. As the ball-end and fillet-end mills are generally used for finish machining, the system is applicable for both cutters. Given a point-based surface represented by a grid of surface points, the system carries out an error analysis on the triangles generated from the rectangular grid of points using an initial choice of the largest tool (ICLT) selected from the cutting tool library in order to check the adequacy of the point density. The system refines the triangular data points until the computed error limits within tolerance. For the ball-end mill selection, the largest radius of the ball-end mill is considered as the ICLT whereas the largest corner radius of the fillet-end mill is considered as the ICLT for the fillet-end mill selection because they provide the maximum machining efficiency in terms of cutter path length. It is noted that the fillet-end mill with larger bottom-disk radius is considered as the ICLT only when the two fillet-end mills have the same corner radius because the cutter with the larger bottom-disk radius provides higher cutting speed. In order to utilise the maximum material removal rate, the list of cutting tool from cutting tool library tools is to be arranged in the following hierarchy order based on the cutter radius R for ball-end mill and bottom-disk radius R_1, corner radius R_2 for the fillet-end mill:

For ball-end mill:

$$C_0\left(R^0\right), C_1\left(R^1\right), \ldots, C_i\left(R^i\right), C_{i+1}\left(R^{i+1}\right), \ldots, C_n\left(R^n\right) \quad \text{for} \quad (i = 0, 1, \ldots, n)$$

where $R^i > R^{i+1}$

For fillet-end mill:

$$C_0\left(R_1^0, R_2^0\right), C_1\left(R_1^1, R_2^1\right), \ldots, C_1\left(R_1^i, R_2^i\right), C_{i+1}\left(R_1^{i+1}, R_2^{i+1}\right), \ldots, C_n\left(R_1^n, R_2^n\right) \quad \text{for} \quad (i = 0, 1, \ldots, n)$$

where $R_2^i > R_2^{i+1}$ and when $R_2^i = R_2^{i+1}$ then only $R_1^i > R_1^{i+1}$

The local gouging due to the cutter bottom is checked and then the checking of global gouging due to the cutter body length is performed. Starting with the largest cutter radius and/or corner radius from the tool library, the local and global gouging are checked and if it fails to do gouge-free machining then the next cutter from the arranged tool library is considered. When the entire surface is gouge-free with the chosen cutting tool then the tool becomes the optimum cutting tool for the given tool library.

Intuitively, the accuracy of cutting tool selection for the point-based surface depends on the density of the surface points. Therefore, the point density checking is essential for accurate estimation of the tool size.

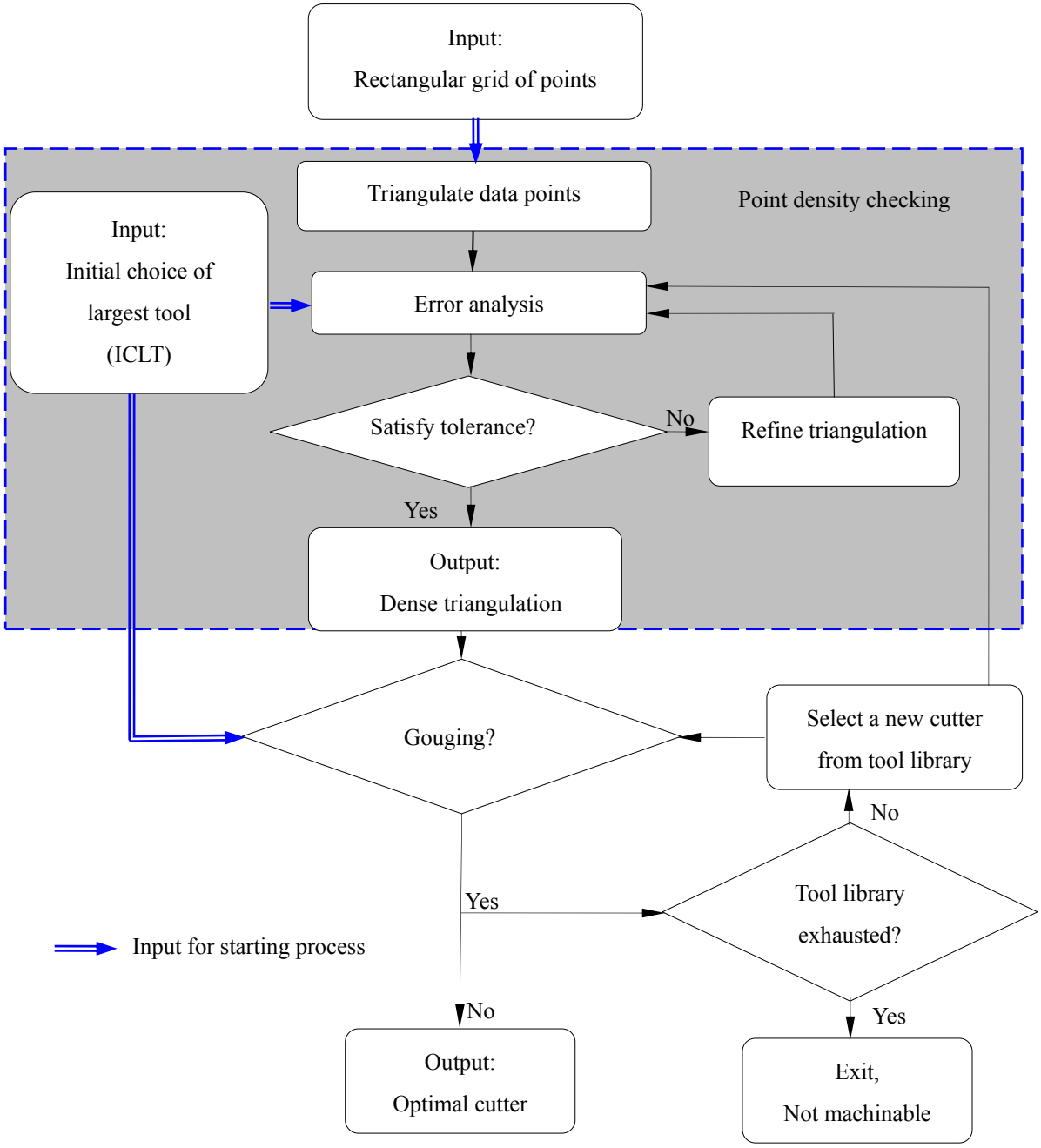

Fig.3. Proposed cutting tool selection system

4. Point density checking

The density of the surface points plays a major role in the accuracy of the tool size estimation for the point-based surface [17]. In this section, an error analysis is performed for the point density checking. The discrete representation of surface introduces error in two ways [8]: the surface error and cutter error. The surface error is the difference between the surface and triangular approximation, and can be computed using the radii of curvature at every surface point based on the circle fitting formula and triangle edge length. The procedure for evaluation of the surface error is presented in [8]. The cutter error is the protrusion of the cutter into the triangle plane. Kayal[8] determines the ball-end mill centre when the spherical part of the cutter touches the three vertices of a triangle and the cutter error is determined as the deviation of the spherical surface from the triangle edges within the triangle boundary. Kayal [21] also presents a method where the fillet-end mill centre is determined when the toroidal surface touches the three vertices of triangle. The cutter error is determined in the triangle normal direction by solving non-linear equations. The total error is a combination of the surface error and cutter error but the nature of the combination depends on the local surface shape, as illustrated in the three configurations of figure 4, and enables to choose appropriate dense set of surface points so that the accuracy of the determined cutter size can be obtained within tolerance.

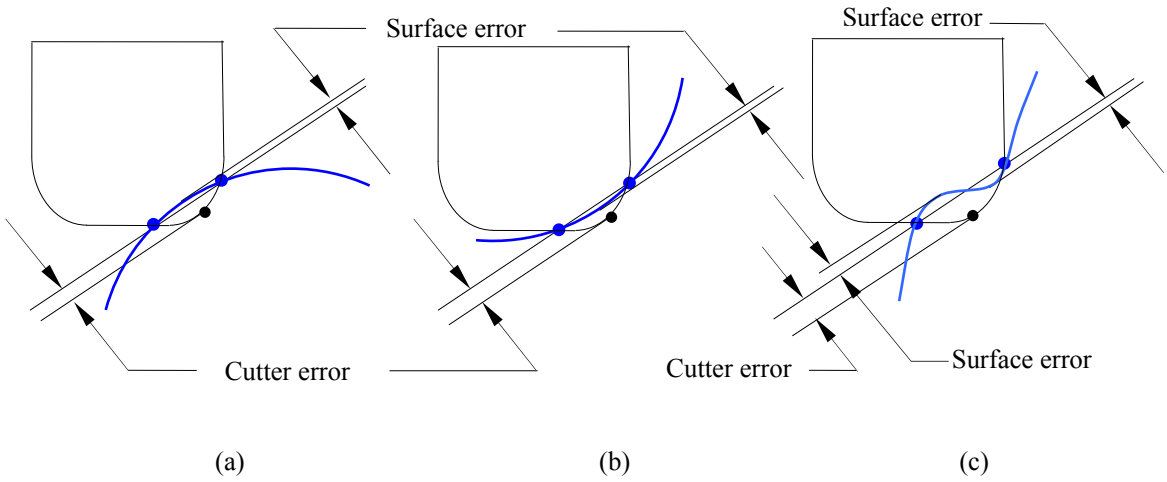

Fig. 4. Combined effect of surface error and cutter error

Given an initial grid of data, an interpolatory subdivision scheme is required to insert extra data points between the existing surface points. There are a number of such algorithms available: quintic interpolation based on arc-length parameterisation [22], four-point interpolatory subdivision proposed by Dyn *et al.* [23] and interpolation based on the Generalised Cornu Spiral [24]. The rectangular grid of surface points can be refined using a suitable subdivision scheme so that it is sufficiently dense to

determine the cutter size accurately within tolerance. For simplicity, the grids of discrete points used in the example have been sampled from parametric surface definition but the algorithms are equally applicable to any grid of points with any subdivision scheme [8]. The initial data point is to be refined until it satisfies a specified tolerance. The gouge checking is performed on a set of triangles generated from a dense rectangular grid of surface points in the following section.

5. Gouge checking

While removing material around the cutter contact point (CC-point), the cutter may interfere another surface point due to the cutter bottom or any other part of the tool body. This interference is called the gouging. The interference with the cutter bottom is called the local gouging and the interaction with the tool body is called the global gouging. Conventionally, the gouging is checked after the entire tool paths have been computed [16]. Ideally, the gouging should be detected in the early stages of cutter path planning. In this paper, a unique approach is therefore proposed, wherein the gouging is checked on a dense set of triangles generated from a rectangular grid of surface points without need to generate cutter paths. The main thrust of the argument is that the tool path generation algorithm must calculate the position of the cutting tool such that it touches the surface at one or more points, and does not protrude the surface anywhere, and this basic procedure must be repeated several times to machine the entire surface. Given three vertices of a triangle, the cutter position is determined using a specified tool type and size in order to check the gouging in the following sub-section:

5.1 Cutter position

There are many methods of CNC machining in terms of machine axis numbers and tool shape, type and orientation. In 3-axis CNC machining, the machine tool simultaneously controls the relative movement between the part and the cutter along its three primary axes, x-, y -, and z-axis. In 5-axis CNC machine, two continuous rotations are synchronised with the x-, y-and z- axis movements and these motions are applied to the cutter spindle, the machine table or sometimes to both. In the point-based approach, the CL-points are computed considering the points under the CC-region where the material removal takes place. As the cutting takes place only in the CC-region which is respectively the spherical and toroidal parts of the ball-end and fillet-end mills, the cutter position is determined by placing the spherical and toroidal parts of the respective cutters to the surface points. Assuming that the cutter axis is parallel to the z-axis for 3-axis CNC machining, the cutter is placed in such a way that three vertices $\mathbf{P}_1(x_1, y_1, z_1), \mathbf{P}_2(x_2, y_2, z_2)$ and $\mathbf{P}_3(x_3, y_3, z_3)$ of a triangle touches the spherical part of the cutter ($z_1 \le c \le z_3 + R$). The a, b, c components of the cutter centre $\mathbf{C}(a, b, c)$ of the ball-end mill of radius R

are then given by [8]:

$$c = \max\left\{\frac{-\alpha_2 \pm \sqrt{\alpha_2^2 - 4\alpha_1\alpha_3}}{2\alpha_1}\right\} \tag{7}$$

$$a = \frac{2c(z_3y_1 - z_1y_3) + y_3\left(x_1^2 + y_1^2 + z_1^2\right) - y_1\left(x_3^2 + y_3^2 + z_3^2\right)}{2(x_1y_3 - y_1x_3)} \tag{8}$$

$$b = \frac{2c(x_3z_1 - x_1z_3) - x_3\left(x_1^2 + y_1^2 + z_1^2\right) + x_1\left(x_3^2 + y_3^2 + z_3^2\right)}{2(x_1y_3 - y_1x_3)} \tag{9}$$

where, $\alpha_1, \alpha_2, \alpha_3$ are given by:

$$\alpha_1 = 4\left\{(z_3y_1 - z_1y_3)^2 + (x_3z_1 - x_1z_3)^2 + (x_1y_3 - y_1x_3)^2\right\}$$

$$\alpha_2 = 4\left\{\begin{array}{l}(z_3y_1 - z_1y_3)\left(y_3\left(x_1^2 + y_1^2 + z_1^2\right) - y_1\left(x_3^2 + y_3^2 + z_3^2\right)\right) \\ +(x_3z_1 - x_1z_3)\left(-x_3\left(x_1^2 + y_1^2 + z_1^2\right) + x_1\left(x_3^2 + y_3^2 + z_3^2\right)\right)\end{array}\right\}$$

$$\alpha_3 = \left\{\begin{array}{l}\left(y_3\left(x_1^2 + y_1^2 + z_1^2\right) - y_1\left(x_3^2 + y_3^2 + z_3^2\right)\right)^2 \\ +\left(-x_3\left(x_1^2 + y_1^2 + z_1^2\right) + x_1\left(x_3^2 + y_3^2 + z_3^2\right)\right)^2 - 4R^2(x_1y_3 - y_1x_3)^2\end{array}\right\}$$

Similarly, when the three triangle vertices $\mathbf{P}_1(x_1, y_1, z_1)$, $\mathbf{P}_2(x_2, y_2, z_2)$ and $\mathbf{P}_3(x_3, y_3, z_3)$ touches the toroidal part (CC-region) of a fillet-end mill having the bottom-disk radius R_1 and corner radius R_2, the a, b, c components of the cutter centre $\mathbf{C}(a, b, c)$ are given by [21]:

$$c = \max\{\beta_1, \beta_2\} \tag{10}$$

$$a = \frac{\begin{array}{l}-y_1x_3^2 - y_1y_3^2 - y_1\left(R_1 + \sqrt{R_2^2 - c^2}\right)^2 + y_1\left(R_1 + \sqrt{R_2^2 - (z_3 - c)^2}\right)^2 + \\ y_3x_1^2 + y_3y_1^2 - y_3\left(R_1 + \sqrt{R_2^2 - (z_1 - c)^2}\right)^2 + y_3\left(R_1 + \sqrt{R_2^2 - c^2}\right)^2\end{array}}{2(x_1y_3 - y_1x_3)} \tag{11}$$

$$b = \frac{\begin{array}{l}-x_3x_1^2 - x_3y_1^2 - x_3\left(R_1 + \sqrt{R_2^2 - c^2}\right)^2 + x_3\left(R_1 + \sqrt{R_2^2 - (z_1 - c)^2}\right)^2 + \\ x_1x_3^2 + x_1y_3^2 - x_1\left(R_2 + \sqrt{R_2^2 - (z_3 - c)^2}\right)^2 + x_1\left(R_1 + \sqrt{R_2^2 - c^2}\right)^2\end{array}}{2(x_1y_3 - y_1x_3)} \tag{12}$$

where, β_1, β_2 are given by:

$$\beta_1, \beta_2 = \text{two roots of} = \left\{ \begin{array}{l} -y_1 x_3^2 - y_1 y_3^2 - y_1 \left(R_1 + \sqrt{R_2^2 - c^2} \right)^2 + y_1 \left(R_1 + \sqrt{R_2^2 - (z_3 - c)^2} \right)^2 + \\ y_3 x_1^2 + y_3 y_1^2 - y_3 \left(R_1 + \sqrt{R_2^2 - (z_1 - c)^2} \right)^2 + y_3 \left(R_1 + \sqrt{R_2^2 - c^2} \right)^2 \end{array} \right\}^2$$

$$+ \left\{ \begin{array}{l} -x_3 x_1^2 - x_3 y_1^2 - x_3 \left(R_1 + \sqrt{R_2^2 - c^2} \right)^2 + x_3 \left(R_1 + \sqrt{R_2^2 - (z_1 - c)^2} \right)^2 + \\ x_1 x_3^2 + x_1 y_3^2 - x_1 \left(R_2 + \sqrt{R_2^2 - (z_3 - c)^2} \right)^2 + x_1 \left(R_1 + \sqrt{R_2^2 - c^2} \right)^2 \end{array} \right\}^2$$

$$- 4 \left(R_1 + \sqrt{R_2^2 - c^2} \right)^2 (x_1 y_3 - y_1 x_3)^2 = 0$$

within the allowable range $(z_1 \le c \le z_3 + R_2)$

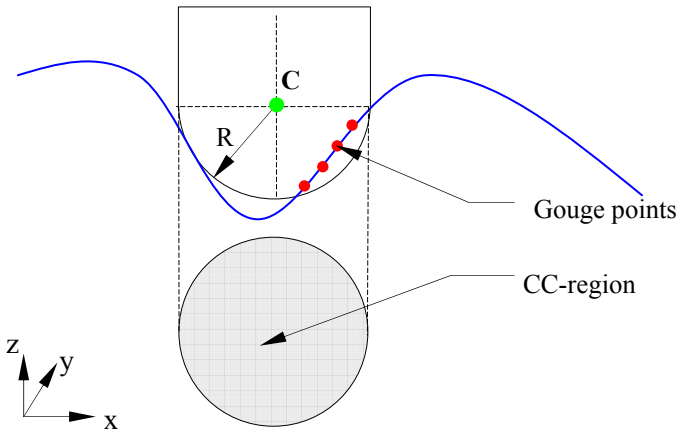

Fig. 5. Local gouging of ball-end mill

5.2 Local gouging

When one edge of the cutter machines the surface at a cutter contact (CC) point, the other part of the cutter bottom may interfere the surface points. This interference is called the local gouging. In order to check the local gouging for a ball-end mill, the distances from all the points within the CC-region as shown in figure 5 is checked. For the cutter position of $\mathbf{C}(a, b, c)$ determined from Eqs. (7-9), the $\mathbf{P}(x, y, z)$ the condition of gouging is derived from the equation of sphere:

$$(x-a)^2 + (y-b)^2 + (z-c)^2 > R^2 \qquad \text{for} \quad (x-a)^2 + (y-b)^2 \le R^2 \qquad (13)$$

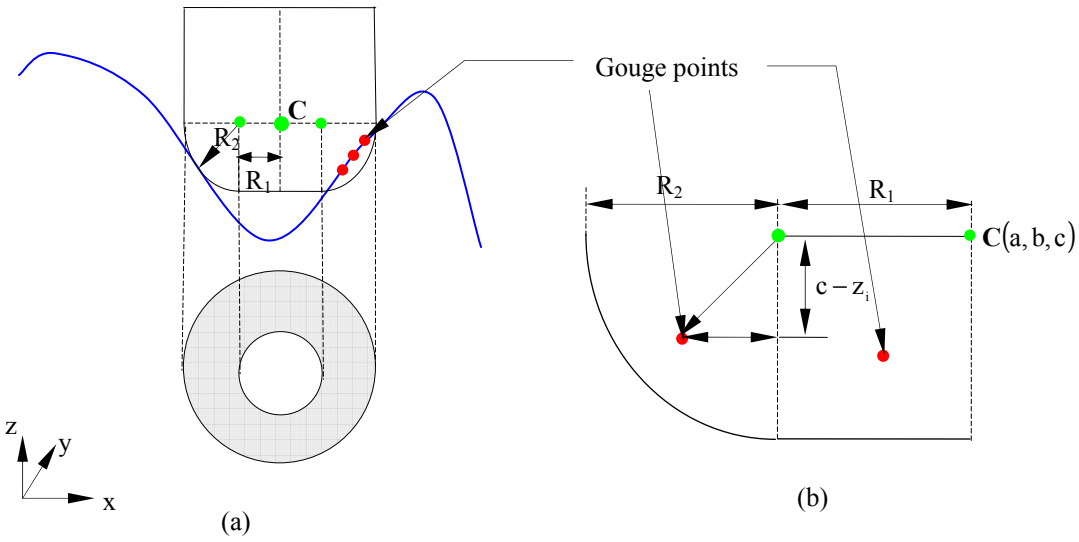

Fig. 6. Local gouging of fillet-end mill

For the fillet-end mill, two radii R_1 and R_2 are responsible to cause the local gouging. For 3-axis CNC machining with the cutter-axis parallel to the z-axis, the local gouging is possible only within the cutter projected area, as shown in figure 6(a). The fillet-end mill centre is determined from Eqs. (10-12) and the condition that the $\mathbf{P}(x,y,z)$ gouges the cutter bottom is then derived according to figure 6(b):

$$z > c - R_2 \qquad \text{for} \quad (x-a)^2 + (y-b)^2 \le R_1^2 \tag{14}$$

$$\left\{\sqrt{(x-a)^2 + (y-b)^2} - R_1\right\}^2 + (z-c)^2 < R_2^2 \qquad \text{for} \quad R_1^2 \le (x-a)^2 + (y-b)^2 \le (R_1 + R_2)^2 \tag{15}$$

5.3 Global gouging

Global gouging refers to the interference of the cutter body including spindles or fixtures with the part surface. In order to avoid global gouging, it is necessary to chose appropriate sizes of neck length, neck diameter and overall length. In some cases, even if the tool is accessible to the entire surface, the tool cannot enter into some regions because of smaller tool body length. This is due to the tool body which collides with the other surface points. Thus tool body collision poses a constraint to the finish machining.

In this paper, the tool body has been abstracted as a series of stacked cylinders/cones due to symmetry. Figure 7 shows the different parts of the tool consisting of neck cylinder of length L_1 and diameter D_1, cone of length L_2 and two diameters D_2, D_3, and shank cylinder of length L_3 and diameter D_3. Given a cutter position $\mathbf{C}(a,b,c)$ determined in sub-section 5.1, the global gouging of a surface point

$\mathbf{P}(x,y,z)$ with the part of the tool body can be checked by determining the shortest distance from the surface points to the cutter axis. In order to find the distance from the cutter axis, the geometric equation of the cutter axis is to be evaluated. There is a problem for determining the equation of the cuter axis. As the x-, y-coordinate are the same, the equation of the cutter axis cannot be determined straightforward without transforming the coordinate system. Without loss of generality, the axis and surface points are therefore rotated by angles α, β, γ respectively about the x-, y-, z-axis in such a way that $\mathbf{C}(a,b,c)$, $\mathbf{P}(x,y,z)$ are transformed to $\mathbf{C}(a',b',c')$, $\mathbf{P}(x',y',z')$ respectively:

$$\begin{pmatrix} a' \\ b' \\ c' \end{pmatrix} = \begin{pmatrix} a\cos\gamma\cos\beta\cos\alpha - a\sin\gamma\sin\alpha + b\cos\gamma\cos\beta\sin\alpha + b\sin\gamma\cos\alpha - c\cos\gamma\sin\beta \\ -a\sin\gamma\cos\beta\cos\alpha - a\cos\gamma\sin\alpha - b\sin\gamma\cos\beta\sin\alpha + b\cos\gamma\cos\alpha + c\sin\gamma\sin\beta \\ a\sin\beta\cos\alpha + b\sin\beta\sin\alpha + c\cos\beta \end{pmatrix} \tag{16}$$

$$\begin{pmatrix} x' \\ y' \\ z' \end{pmatrix} = \begin{pmatrix} x\cos\gamma\cos\beta\cos\alpha - x\sin\gamma\sin\alpha + y\cos\gamma\cos\beta\sin\alpha + y\sin\gamma\cos\alpha - z\cos\gamma\sin\beta \\ -x\sin\gamma\cos\beta\cos\alpha - x\cos\gamma\sin\alpha - y\sin\gamma\cos\beta\sin\alpha + y\cos\gamma\cos\alpha + z\sin\gamma\sin\beta \\ x\sin\beta\cos\alpha + y\sin\beta\sin\alpha + z\cos\beta \end{pmatrix} \tag{17}$$

If another point $\mathbf{C}'(a,b,h)\ (h \neq 0)$ is chosen on the cutter axis in the original coordinate system, the shortest distance between the cutter axis and $\mathbf{P}(x',y',z')$ is given by:

$$d_{PA} = \left\| \frac{\begin{vmatrix} \mathbf{i} & \mathbf{j} & \mathbf{k} \\ -c\cos\gamma\sin\beta + h\cos\gamma\sin\beta & c\sin\gamma\sin\beta - h\sin\gamma\sin\beta & c\cos\beta - h\cos\beta \\ \Delta x & \Delta y & \Delta z \end{vmatrix}}{\sqrt{(-c\cos\gamma\sin\beta + h\cos\gamma\sin\beta)^2 + (c\sin\gamma\sin\beta - h\sin\gamma\sin\beta)^2 + (c\cos\beta - h\cos\beta)^2}} \right\| \tag{18}$$

where, i, j, k are unit vectors in x, y, z directions respectively.

$$\Delta x = (x-a)\cos\gamma\cos\beta\cos\alpha - (x-a)\sin\gamma\sin\alpha + (y-b)\cos\gamma\cos\beta\sin\alpha + (y-b)\sin\gamma\cos\alpha - (z-c)\cos\gamma\sin\beta$$

$$\Delta y = -(x-a)\sin\gamma\cos\beta\cos\alpha - (x-a)\cos\gamma\sin\alpha - (y-b)\sin\gamma\cos\beta\sin\alpha + (y-b)\cos\gamma\cos\alpha + (z-c)\sin\gamma\sin\beta$$

$$\Delta z = (x-a)\sin\beta\cos\alpha + (y-b)\sin\beta\sin\alpha + (z-c)\cos\beta$$

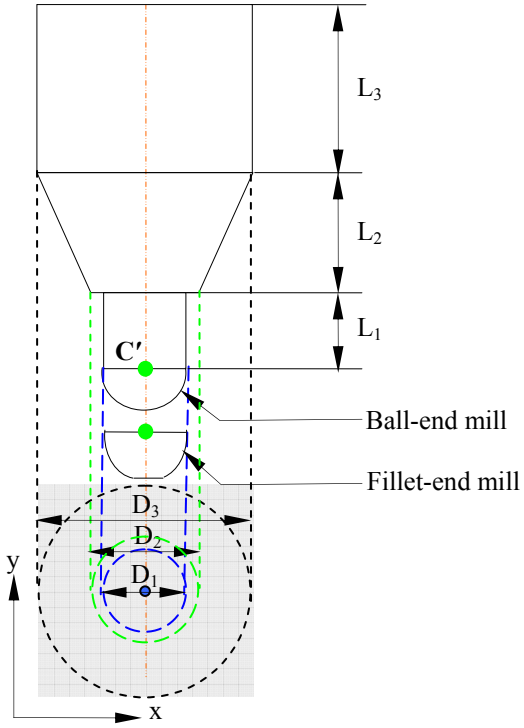

Fig. 7. Tool dimensions considered for global gouging

Given a cutter position $\mathbf{C}(a',b',c')$ determined from Eq. (16), the conditions of the global gouging for the $\mathbf{P}(x',y',z')$ obtained from Eq. (17) are then derived based on the geometric property of a cylinder and cone using the shortest distance evaluated according to Eq. (18):

$$d_{PA} < \frac{D_1}{2} \quad \text{for} \quad (x'-a')^2+(y'-b')^2 \le \frac{D_1^2}{4} \quad \text{and} \quad z' \ge c'+L_1 \tag{19}$$

$$d_{PA} < \frac{D_2}{2} \quad \text{for} \quad \frac{D_1^2}{4} \le (x'-a')^2+(y'-b')^2 \le \frac{D_2^2}{4} \quad \text{and} \quad z' \ge c'+L_1 \tag{20}$$

$$d_{PA} < \frac{D_2}{2}+(z'-c'-L_1)\left(\frac{D_3-D_2}{2L_2}\right) \quad \text{for} \frac{D_2^2}{4} \le (x'-a')^2+(y'-b')^2 \le \frac{D_3^2}{4} \text{ and}$$

$$c'+L_1 \le z' \le c'+L_1+L_2 \tag{21}$$

$$d_{PA} < \frac{D_3}{2} \quad \text{for} \quad \frac{D_2^2}{4} \le (x'-a')^2+(y'-b')^2 \le \frac{D_3^2}{4} \text{ and } z' \ge c'+L_1+L_2 \tag{22}$$

6. Machining examples

The proposed cutter selection algorithm is applied in two examples. The first example is a point-based model (shown in figure 8) that is generated from the surface model consisting of 3×2 bi-cubic Bézier patches. These patches consist of doubly convex, doubly concave and saddle type surfaces and the entire model is machinable using a 3-axis CNC machine. The local gouging and global gouging are checked respectively using Eqs. (13-15) and Eqs. (19-22) on the triangles generated from the rectangular grid of surface points.

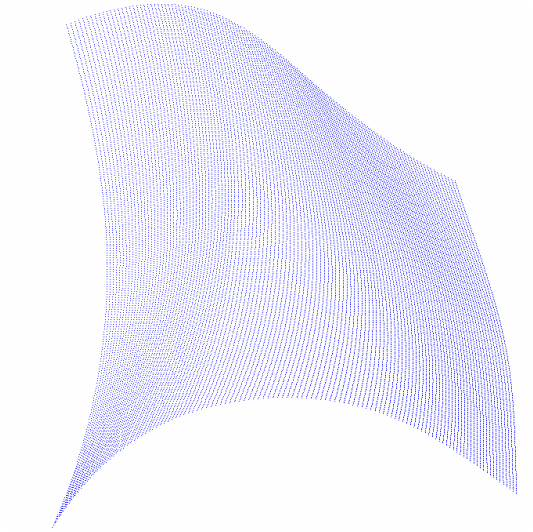

Fig. 8. Point-based model of 3×2 Bézier surface

Tool no.	R (mm)	D_1 (mm)	D_2 (mm)	D_3 (mm)	L_1 (mm)	L_2 (mm)	L_3 (mm)
B_1	12.5	25	25	25	55	2	125
B_2	10	20	20	20	38	2	122
B_3	9	18	18	16	34	2	106
B_4	8	16	16	16	30	2	110
B_5	7.5	15	15	16	30	2	110
B_6	7	14	14	12	26	2	94
B_7	6	12	12	12	22	2	88
B_8	5	10	10	10	18	2	82
B_9	4.5	9	9	10	18	2	82
B_{10}	4	8	8	8	14	2	86
B_{11}	3.5	7	7	8	14	2	86
B_{12}	3	6	6	6	12	2	68
B_{13}	2.5	5	5	6	12	2	68
B_{14}	2	4	4	6	8	4	62
B_{15}	1.5	3	3	6	8	6	62
B_{16}	1.25	2.5	2.5	6	6	6.5	54
B_{17}	1	2	2	6	6	7.5	54

Table 1. Tool library for ball-end mills

A list of cutters given in Table 1 is used for the ball-end mill selection. The tool selection is started with a tool no. B_1 of R = 12.5 mm on a (111×61) grid of surface points that estimates the total error for point density checking 0.0092 mm and it is observed that the tool gouges 32226 data points. Then tool no. B_2 of R = 10.0 mm gouges 1616 data points for a (111×61) grid of surface points that estimates the total error 0.0108 mm. Even tool no. B_3 of R = 9.0 mm gouges 180 data points on a (121×71) grid of surface points that estimates the total error 0.0089 mm. Finally, tool no. B_4 of R = 8.0 mm does not gouge any data point for a (121×71) grid of surface points that estimates total error 0.0097 mm. Therefore, tool no. B_4 of R = 8.0 mm becomes the optimum tool for the tool library given in Table 1.

Tool no.	**R_1 (mm)**	**R_2 (mm)**	**D_1 (mm)**	**D_2 (mm)**	**D_3 (mm)**	**L_1 (mm)**	**L_2 (mm)**	**L_3 (mm)**
F_1	1	5	12	11.85	12	12	24	74
F_2	2	4	12	11.85	12	12	24	74
F_3	1	4	10	09.85	10	10	20	70
F_4	3	3	12	11.85	12	12	24	74
F_5	2	3	10	09.85	10	10	20	70
F_6	1	3	08	07.85	08	08	16	66
F_7	4	2	12	11.85	12	12	24	74
F_8	3	2	10	09.85	10	10	20	70
F_9	2	2	08	07.85	08	08	16	66
F_{10}	1	2	06	05.85	06	06	12	52
F_{11}	5	1	12	11.85	12	12	24	74
F_{12}	4	1	10	09.85	10	10	20	70
F_{13}	3	1	08	07.85	08	08	16	66
F_{14}	2	1	06	05.85	06	06	12	52
F_{15}	1	1	04	03.96	06	04	26	40

Table 2. Tool library for fillet-end mills

The fillet-end mill selection is performed for the model shown in figure 8 using a list of cutters given in Table 2. The selection is started with tool no. F_1 of R_1 = 1.0 mm, R_2 = 5.0 mm for a (131×81) grid of surface points that estimates the total error for point density checking 0.0107 mm and it is found that the tool does not gouge any surface point. Therefore, tool no. F_1 is the optimum fillet-end mill for the given tool library.

As an industrial example, the shoe last model consisting of 120 bi-cubic Bezier surface is considered. Figure 9 shows the point-based model of the shoe last supplied by Clarks International, which is chosen because it consists of several doubly curved free-form surfaces, but it does not contain pocket areas, planar surfaces or irregular topologies. The algorithm of cutter selection is applied on the shoe-last model and tool no. F_1 becomes the optimal tool which does not gouge any surface point. The surface textures and machining times are measured to compare the relative performance of different tool sizes on machining. The other two cutting tools namely tool nos. F_2 and F_3 are therefore considered. The tolerances for the point density checking, cutter path planning and gouge checking along with the different cutting speeds are given in Table 3. The step-forward and step-interval distances are determined

adaptively in such a way that the machined surface error which is the combined effect of chordal deviation and cusp height is limited within tolerance 0.01 mm

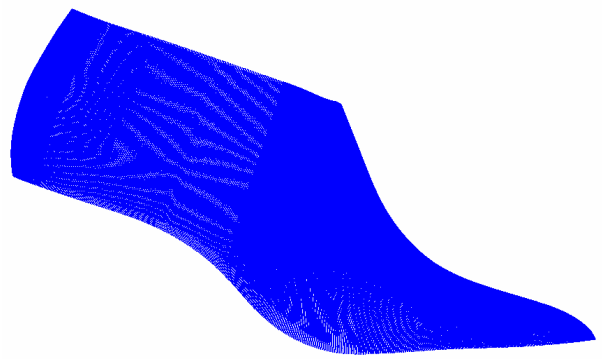

Fig. 9. Point-based model of shoe-last supplied by Clarks International

The part of the shoe last model is machined with a Hermle C600U 5-axis machining centre equipped with a Heidenhain TNC430 controller using the feed rate 2000 mm/min and spindle speed 3000 rpm. The material used for machining is Cibatool board material BM 5460. The surface finish from raster milling has been compared to polyhedral machining using PowerMILL, a commercial software developed by Delcam Plc. The surface texture of three machined shoes is sampled with the *Hobson TalyMap* instrument for the tangent continuous regions, and measured in terms of the roughness and waviness using *TalyMap Universal* software. It has been observed that three shoes produce the same level of surface finish and the finished surfaces are comparable in quality to polyhedral machined surfaces. It is seen from Table 3 that the machining time is the least for the tool no. F_1 and therefore, this is the optimal tool size for the tool library given in Table 2. Thus the cutting tool selection algorithm enables to limit the machined surface error within tolerance, and minimises the machining time.

	Tool no. F_1	**Tool no. F_2**	**Tool no. F_3**
Tolerance for point density checking (mm)	0.01	0.01	0.01
Tolerance for adaptive cutter path planning (mm)	0.01	0.01	0.01
Tolerance for gouge checking (mm)	0.01	0.01	0.01
Rapid feed (mm/min)	4000	4000	4000
Plunge feed (mm/min)	2000	2000	2000
Cutting speed (mm/min)	2000	2000	2000
Spindle speed (rpm)	3000	3000	3000
Estimated machining time (sec)	632	675	672
Actual machining time (sec)	795	889	854

Table 3. Machining parameters for three tools

7. Conclusions

An optimal cutter selection algorithm for the ball-end and fillet-end mills has been proposed for any 3D free-form surface defined by a set of surface points. The algorithm is limited to a 3-axis CNC machine for finish machining. The proposed method chooses an optimal cutter from the list of cutters available in a standard cutting tool library in such a way that the point-based surface is machined with the largest cutter in terms of cutter radius and/or corner radius without gouging any surface point. A unique algorithm of the local and global gouging is presented for finish machining of the point-based surface. Given three vertices of a triangle generated from a rectangular grid of surface points that represents the point-based surface, a unique cutter position is determined using a specified tool type, size and then the gouging is checked whether the cutter interferes with any neighbourhood data point. The distance between the cutter bottom and surface points is used for the local gouging and the shortest distance between the cutter axis and surface points is used to detect the global gouging. Thus the proposed algorithm enhances the machining efficiency without compromising the machined surface quality.

The machining efficiency could be increased using multiple cutters for different regions based on the geometric features of the surface, which is certainly an area of the author's future research. The challenging issues are to decompose the surface into different regions and determine the optimum tool sizes for respective regions. Then generating cutter paths for all regions with their respective optimum tool sizes and linking respective tool paths from one region to another without pronounced tool marks left at the boundary are the author's future research work.

Acknowledgements

The author has been motivated to write this paper for the expert comments given by Prof A Ball and Dr M Loftus, Mechanical Engineering, University of Birmingham, UK, and express deep gratitude to the reviewers for valuable comments/suggestions.

References

1. Chen, Z.C., Vickers, G.W., and Dong, Z. (2004), A new principle of CNC tool path generation for three-axis sculptured part machining – a steepest-ascending tool path, *Journal of Manufacturing Science and Engineering,* 126, 515-523.

2. Lee, S.G., and Yang, S.H. (2002), CNC Tool-path planning for high speed high resolution machining using a new tool-path calculation algorithm, *International Journal of Advanced Manufacturing*

Technology, 20, 326-333.

3. Lai, X.D., Zhou, Y.F., Zhou, J., Peng, F.Y., and Yan, S.J. (2003), Geometric error analysis and control for 5-axis machining of large sculptured surfaces, *International Journal of Advanced Manufacturing Technology*, 21, 110-118.

4. Park, S.C., and Chung, Y.C. (2003), Tool-path generation from measured data, *Computer-Aided Design*, 35, 467-476.

5. Rao, N., Ismail, F., and Bedi, S. (1997), Tool path planning for five-axis machining using the principal axis method, *International Journal of Machine Tools and Manufacture*, 37, 1025-1040.

6. Flutter, A., and Todd, J. (2001), A machining strategy for toolmaking, *Computer-Aided Design*, 33, 1009-1022.

7. Gray, P., Bedi, S., and Ismail, F. (2003), Rolling ball method for 5-axis surface machining, *Computer-Aided Design*, 35, 347-357.

8. Kayal, P. (2007), Offset error analysis of ball-end mill for cutter path generation from point-based surfaces, *International Journal of Advanced Manufacturing Technology*, (press)

9. Feng, H.Y., and Teng, Z. (2005), Iso-planar piecewise NC tool path generation from discrete measured data points, *Computer-Aided Design*, 37, 55-64.

10. Sarma, R., and Dutta, D. (1996), Machining surfaces composed of cyclide patches, *Computers in Industry*, 31, 129-142**.**

11. Lee, Y.S., and Chang, T.C. (1996), Automatic cutter selection for 5-axis sculptured surface machining,. *International Journal of Production Research*, 34, 977-998.

12. Bala, M. and Chang, T.C. (1991), Automatic cutter selection and optimal cutter path generation for prismatic parts, *Internal Journal of Production Research*, 29, 2163-2176.

13. Yao, Z., Gupta, S.K., and Nau, D.S. (2003), Algorithm for selecting cutters in multi-part milling problems, *Computer-Aided Design*, 35, 825-839.

14. Yang, D.C.H., and Han, Z. (1999), Interference detection and optimal tool selection in 3-axis NC machining of free-form surfaces, *Computer Aided Design*, 31, 303-315.

15. Glaeser, G., Wallner, J., and Pottmann, H. (1999), Collision-free 3-axis milling and selection of cutting tools, *Computer Aided Design*, 31, 225-232.

16. Jensen, C.G., Red, W.E., and Pi, J. (2002), Tool selection for five-axis curvature matched machining, *Computer-Aided Design*, 34, 251-266.

17. OuYang, D., Nest, B.A.V., Feng, H.Y. (2005), Determining gouge-free ball-end mills for 3D surface machining from point data, *Robotics and Computer-Integrated Manufacturing*, 21, 338-345.

18. Kayal, P. (2007), Inverse offset method for adaptive cutter path generation from point-based surface, *International journal of CAD/CAM*, 7, 1-18.

19. Marciniak, K. (1991), Geometric Modelling for Numerically Controlled Machining, Oxford University press.

20. Lo, C.C. (2000), Two stage cutter-path scheduling for ball-end milling of concave and wall-bounded surfaces, *Computer-Aided Design*, 32, 597-603.

21. Kayal, P. (2007), A point-based approach for cutter path generation using fillet-end mill, *Computer-Aided Design*, (press).

22. Todd, P.H., and McLeod, R.J.Y. (1986), Numerical estimation of the curvature of surfaces, *Computer-Aided Design*, 18, 33-37

23. Dyn, N., Levin, D., and Gregory, J.A. (1987), A 4-point interpolatory sub-division scheme for curve design, *Computer-Aided Geometric Design*, 4, 257-268.

24. Ali, J.M., Tookey, R.M., and Ball, J.V. (1999), The generalised Cornu spiral and its application to span generation, *Journal of Computational and Applied Mathematics*, 102, 37-47.

Author's Biographies

Prasenjit Kayal has a long term engineering and technology development career in offshore, petrochemical, refinery and gas processing industries. His expertise lies on analysis and design methodology development, execution of advanced engineering projects in offshore/onshore pipelines, above/under-ground piping, pressure vessels, tall columns, heat exchangers, etc. He has published several peer reviewed journal papers, and also presented papers in international conferences in India, USA and UK. His scientific interests include geometry-based algorithm for cutter path generation, 3-axis and 5-axis CNC machining, finite element analysis and stress analysis. This work was executed while he was in the School of Engineering (Mechanical), University of Birmingham, UK.